

# Stability enhancement of nanopillar structure for spin transfer magnetization switching using IrMn buffer layer

J. C. Lee

*Department of Physics, Inha University, Incheon 403-751, Korea and Advanced Metals Research Center, Korea Institute of Science and Technology, Seoul 136-791, Korea*

M. G. Chun and W. H. Park

*Advanced Metals Research Center, Korea Institute of Science and Technology, Seoul 136-791, Korea*

C.-Y. You<sup>a)</sup>

*Department of Physics, Inha University, Incheon 403-751, Korea*

S.-B. Choe

*Department of Physics, Seoul National University, Seoul 151-747, Korea*

W. Y. Yung and K. Y. Kim

*Advanced Metals Research Center, Korea Institute of Science and Technology, Seoul 136-791, Korea*

(Presented on 2 November 2005; published online 26 April 2006)

We report here the effect of ultrathin IrMn buffer layer on the magnetic and spin transport properties of spintronic structure for current-induced magnetization switching. The insertion of the ultrathin ( $\sim 1$  nm) IrMn buffer layer drastically enhanced the coercive field of the fixed ferromagnetic layer from 36 to 215 Oe. Interestingly, the ultrathin IrMn buffer layer even enhanced the magnetoresistance ratio about 30%, and consequently the spin polarization effect was enhanced by reducing the critical current density of magnetization switching from  $3.13 \times 10^8$  to  $1.16 \times 10^8$  A/cm<sup>2</sup>. © 2006 American Institute of Physics. [DOI: [10.1063/1.2175726](https://doi.org/10.1063/1.2175726)]

## I. INTRODUCTION

The stability of magnetization states in ferromagnetic/nonmagnetic/ferromagnetic trilayered structures for spin dependent applications, such as giant magnetoresistance and magnetic tunneling junction, has been one of the crucial issues in practical implementation of the applied technology. In many applications, insertion of an antiferromagnetic layer such as FeMn and IrMn provided the drastic enhancement of coercive field of the fixed ferromagnetic layer via the exchange bias from the antiferromagnetic layer. However, it has been reported that the thick antiferromagnetic layer may caused a strong depolarization of the spin current by Jiang *et al.*<sup>1</sup> It thus undesirably inflates the critical current density required for magnetization switching in the current-induced magnetization switching technology.<sup>2-10</sup> Therefore stabilizing mechanism for the fixed ferromagnetic layer is scientifically challenging. Recently, we found that ultrathin ( $\sim 1$  nm) IrMn buffer layer enhanced the coercive field of CoFe layer without degrading the spin polarization. In this paper, we report the effect of the ultrathin IrMn buffer layer on the magnetic and spin polarization properties of the nanofabricated pillar structure for the current-induced magnetization switching.

## II. SAMPLE PREPARATION AND EXPERIMENTAL SETUP

To contradict the effect of ultrathin IrMn buffer layer, we prepared two types of the multilayer films without an IrMn

buffer layer (type I) and with an IrMn buffer layer (type II). The detailed multilayer structure was SiO<sub>2</sub>/Ta(5 nm)/IrMn(1 nm)/CoFe(5 nm)/Cu(3 nm)/CoFe(1 nm)/NiFe(5 nm)/Ta(5 nm). Care was taken to keep the same preparation condition except the IrMn thickness. The layer structure was deposited in an ultrahigh-vacuum sputtering system with a base pressure of  $8.0 \times 10^{-9}$  Torr and the working pressures of 1.0–7.0 mTorr of Ar (purity of 99.9999%) depending on each particular layer. Deposition rate of each layer was kept to 0.5–2.0 Å/s, controlled by the sputtering power and Ar gas pressure. A bias magnetic field of 100 Oe was applied along the film plane during the sputtering to induce a magnetic easy axis. The magnetoresistance and the magnetization hysteresis were characterized by use of a dc four-point probe technique and a vibrating sample magnetometry, respectively, at ambient temperature. The film structure was characterized by the x-ray diffraction technique using a Cu  $K_{\alpha}$  source (RIGAKA Co.), with the scanning over the angle between 20° and 80° with an interval of 0.02°.

The films were further processed to nanopillar structures for the current-induced magnetization switching experiment.<sup>11</sup> The nanostructure was fabricated by a stencil-mask technique. In the technique, the nanometer-sized patterns ( $100 \times 150$  nm<sup>2</sup>) were defined by electron-beam lithography, followed by an ion milling and wet etching process. A 150 nm platinum layer was used for the metal stencil. The multilayer structure was deposited through the stencil on the bottom electrode, and finally the top electrode was added. Two types of the films were prepared without the IrMn buffer layer (type III) and with the IrMn buffer layer (type IV). The detailed structures were CoFe(12 nm)/Cu(6 nm)/

<sup>a)</sup>Electronic mail: cyyou@inha.ac.kr

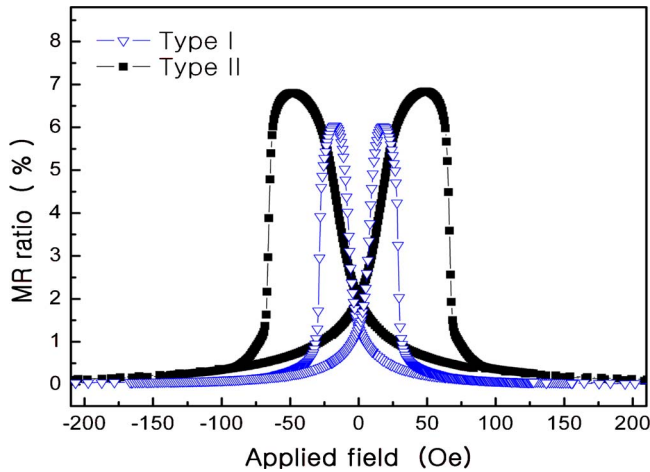


FIG. 1. (Color online) Magnetoresistance curves of type I sample without IrMn buffer layer and type II sample with IrMn buffer layer.

CoFe(3 nm) (type III) and Ta(5 nm)/IrMn(1 nm)/CoFe(6 nm)/Cu(6 nm)/CoFe(3 nm) (type IV). A four-probe dc measurement technique was applied to characterize the magnetoresistance and the magnetization switching properties. The magnetoresistance curves were measured by probing the electric resistance with sweeping the magnetic field applied along the film plane at ambient temperature. To avoid the current-induced effect, the current was kept constant to 1 mA in the direction from the free layer to the fixed layer, during the magnetoresistance measurement. The current-induced magnetization switching properties were characterized by probing the magnetoresistance with sweeping the electric current in the range of  $\pm 50$  mA with a sweeping rate of 1 mA/s. Here, the sign of injected currents was defined as positive when current flowed from the free layer to the fixed layer. A strong magnetic field larger than  $-2$  kOe was applied to saturate the magnetization of a sample, and then a bias magnetic field of the same polarity was kept during the measurement. The bias magnetic field enhances the stability of the antiparallel alignment.

### III. RESULTS AND DISCUSSION

Figure 1 shows the magnetoresistance curves of the unstructured type I and II samples. Both samples showed a larger electric resistance for the antiparallel alignment. Type II sample showed a magnetoresistance ratio (about 6.69%) larger than that (about 5.14%) of type I sample. Figure 2 shows the magnetic hysteresis loops of the samples. Step-wise behavior was ascribed to the different coercive fields of the free and fixed magnetic layers—the inner step came from the switching of the free magnetic layer and the outer came from the fixed magnetic layer. The coercive field of the fixed magnetic layer increased drastically from 36 to 215 Oe, by insertion of the IrMn buffer layer, as intended.

A detailed characterization revealed that there was no unidirectional shift of the hysteresis loop, even though there was a drastic enhancement of the coercive field. The loop shift has been an evidence of the exchange bias from the antiferromagnetic buffer layer. To reveal the nature of the coercive field enhancement without exchange biasing, we

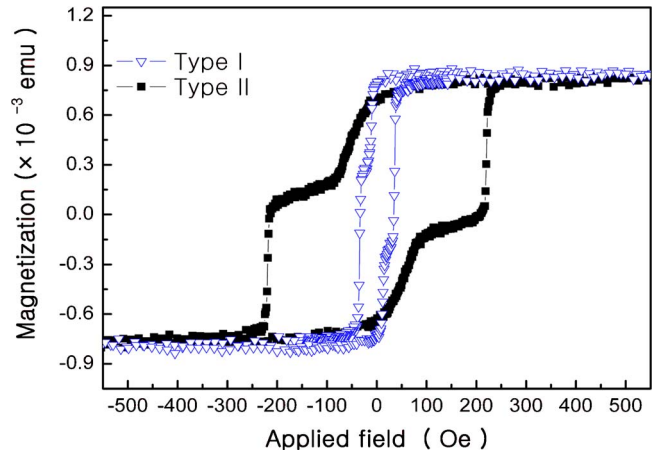


FIG. 2. (Color online) Magnetization hysteresis curves of type I sample without IrMn buffer layer and type II sample with IrMn buffer layer.

characterized the crystalline texture of type II sample, in comparison with another sample labeled as type II'. Type II' sample had basically the same multilayer structure with type II sample, except the inversed layering sequence, i.e., type II' sample was SiO<sub>2</sub>/Ta/NiFe/CoFe/Cu/CoFe/IrMn/Ta while type II sample was SiO<sub>2</sub>/Ta/IrMn/CoFe/Cu/CoFe/NiFe/Ta. Each inversely corresponding layer had the same thickness. Interestingly enough, type II' sample exhibited a finite exchange bias whereas type II sample showed no exchange bias. An x-ray diffraction study revealed that both the samples had the (111) growth orientation, as shown in Fig. 3. However, type II sample showed almost disordered growth phase with a weak (111) diffraction peak, whereas type II' sample showed strong (111) diffraction peak. It was ascribed to the fact that the Ta seed layer enhances the (111) growth texture of NiFe layer.<sup>12,13</sup> We thus conjecture that the disordered phase of the ultrathin IrMn layer on the Ta seed layer was the origin of nonexchange biasing of type II sample. Further detailed characterization is beyond the scope of this paper.

Most interesting feature of the ultrathin disordered IrMn buffer layer was that it did not diffuse the spin polarization, although the thick ordered IrMn antiferromagnetic layer may

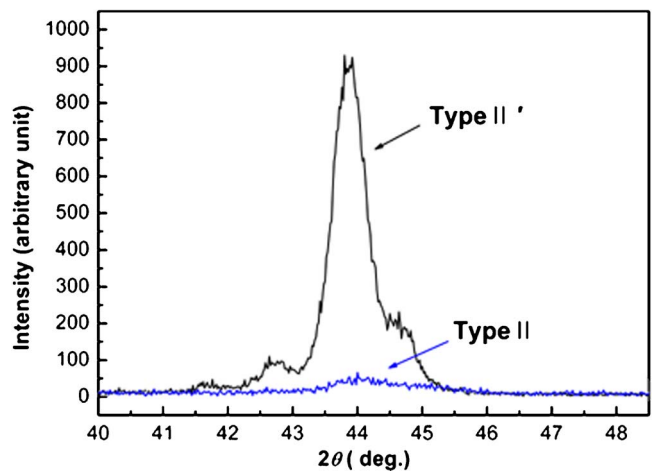


FIG. 3. (Color online) X-ray diffraction peaks of type II sample having no exchange bias and type II' sample exhibiting a finite exchange bias.

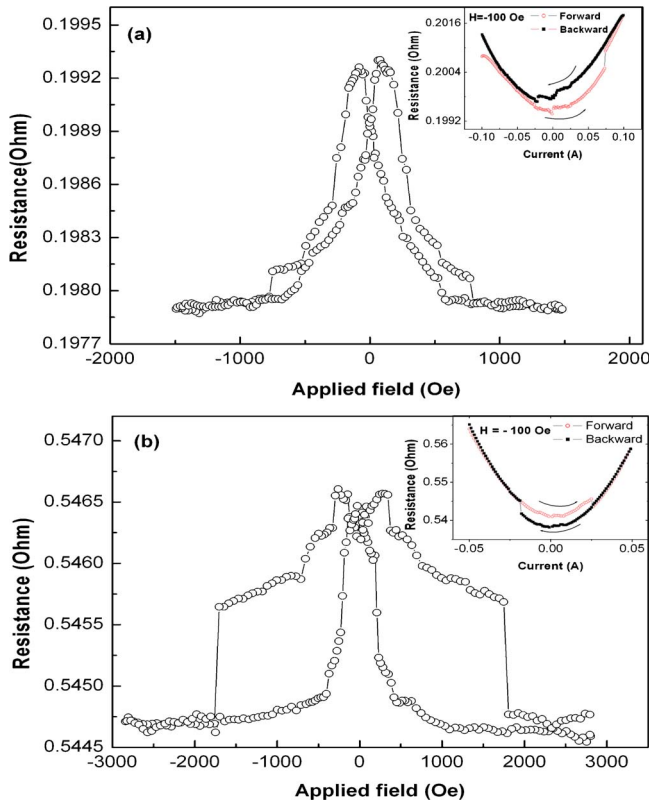


FIG. 4. (Color online) Magnetoresistance curves of (a) type III nanospintronic structure without IrMn buffer layer and (b) type IV nanospintronic structure with IrMn buffer layer. The inset shows the current-induced magnetization switching curves.

diffuse the spin polarization.<sup>1</sup> The spin dependent phenomena were thus unaffected irrespective to the existence of the ultrathin disordered IrMn buffer layer. Figure 4 shows the magnetoresistance curves of the nanospintronic type III and IV samples. Due to the coercive field enhancement of the fixed magnetic layer in type IV sample with the IrMn buffer layer, one could enhance the stability of the fixed magnetic layer during the current-induced switching of the free magnetic layer. The coercive field enhancement would further reduce the chaotic interference between the magnetization of the free and the fixed magnetic layers under a spin current.

The current-induced switching properties were characterized via current versus resistance measurement, as shown in the insets of Fig. 4. The magnitude of resistance jumps in the current-induced switching curve matched to the magnetoresistance ratio, which evidenced the switching of full magnetic alignment of the free magnetic layer. A bias magnetic field of  $-100$  Oe was applied to enhance the stability of the antiparallel alignment. Due to the bias magnetic field, the critical current for magnetization switching became asymmetric: larger positive current  $I^{AP \rightarrow P}$  needed to induce antiparallel to parallel switching while smaller negative current

$I^{P \rightarrow AP}$  needed to induced parallel to antiparallel switching. The average critical current density was defined as  $J_C = (|I^{AP \rightarrow P}| + |I^{P \rightarrow AP}|)/2A$ , where  $A$  is junction area. The estimated  $J_C$  is  $3.13 \times 10^8$  A/cm<sup>2</sup> for type III sample and  $1.16 \times 10^8$  A/cm<sup>2</sup> for type IV sample, respectively. The larger critical current density is a common feature of the CoFe-based trilayers, whereas smaller ones have been reported in the Co-based structures.<sup>1,9,14</sup> It is interesting to note that the critical current density decreased even with an insertion of the IrMn buffer layer, which implied that the ultrathin disordered IrMn buffer layer exhibited no spin diffusion. The physical origin of reduction of critical current density is not yet clear, but one of the possible scenarios is a geometrical effect. The ultrathin disordered IrMn layer has an island formation, so that it generates nonuniform current distribution. It causes strong local current density in some area and reduces the overall switching current.

#### IV. CONCLUSION

The magnetic and the spin polarization properties of the trilayered nanospintronic structure were characterized with respect to the insertion of ultrathin IrMn buffer layer. The ultrathin IrMn buffer layer enhanced the coercive field of the fixed magnetic layer, without increasing the critical current for magnetization switching. The IrMn buffer layer thus meets the two indispensable requirements of stability enhancement without degrading the spin polarization.

#### ACKNOWLEDGMENT

The financial support from the ‘‘R&D Program for NT-IT Fusion Strategy of Advanced Technologies’’ is gratefully acknowledged.

- <sup>1</sup>Y. Jiang, S. Abe, T. Ochiai, T. Nozaki, A. Hirohata, N. Tezuka, and K. Inomata, Phys. Rev. Lett. **92**, 167204 (2004).
- <sup>2</sup>J. C. Slonczewski, J. Magn. Magn. Mater. **159**, L1 (1996).
- <sup>3</sup>L. Berger, Phys. Rev. B **54**, 9353 (1996).
- <sup>4</sup>E. B. Myers, D. C. Ralph, J. A. Katine, R. N. Louie, and R. A. Buhrman, Science **285**, 867 (1999).
- <sup>5</sup>J. A. Katin, F. J. Albert, and R. A. Buhrman, Phys. Rev. Lett. **84**, 3149 (2000); F. J. Albert, J. A. Katine, D. C. Ralph, and R. A. Buhrman, Appl. Phys. Lett. **77**, 3809 (2000).
- <sup>6</sup>X. Waintal, E. B. Myers, P. W. Brouwer, and D. C. Ralph, Phys. Rev. B **62**, 12317 (2000).
- <sup>7</sup>M. D. Stiles and A. Zangwill, Phys. Rev. B **66**, 014407 (2002).
- <sup>8</sup>E. B. Myers, D. C. Ralph, J. A. Katine, R. N. Louie, and R. A. Buhrman, Science **285**, 867 (1999).
- <sup>9</sup>M. Tsoi, A. G. M. Jansen, J. Bass, W. C. Chiang, V. Tsoi, and P. Wyder, Nature (London) **406**, 46 (2000).
- <sup>10</sup>F. J. Albert, N. C. Emley, E. B. Myers, D. C. Ralph, and R. A. Buhrman, Phys. Rev. Lett. **89**, 226802 (2002).
- <sup>11</sup>J. Z. Sun, D. J. Monsma, and T. S. Kuan, J. Appl. Phys. **93**, 5855 (2002).
- <sup>12</sup>M. H. Li, J. W. Cai, G. H. Yu, H. W. Jiang, Y. W. Lai, F. W. Zhu, Mater. Sci. Eng., B **B90**, 296 (2002).
- <sup>13</sup>L. Ritchie, X. Liu, S. Ingvarsson, G. Xia, J. Du, and J. Q. Xiao, J. Magn. Magn. Mater. **247**, 187 (2002).
- <sup>14</sup>T. Y. Chen, Y. Ji, C. L. Chien, and M. D. Stiles, Phys. Rev. Lett. **93**, 026601 (2004).